IOP PUBLISHING JOURNAL OF PHYSICS D: APPLIED PHYSICS

J. Phys. D: Appl. Phys. **44** (2011) 325003 (6pp) doi:10.1088/0022-3727/44/32/325003

Optical properties in the soft photonic crystals based on ferrofluids

C Z Fan[1,3], E J Liang[1] and J P Huang[2]

[1] School of Physical Science and Engineering, and Key Laboratory of Materials Physics of Ministry of Education of China, Zhengzhou University, Zhengzhou 450052, People's Republic of China
[2] Department of Physics, State Key Laboratory of Surface Physics, and Key Laboratory of Micro and Nano Photonic Structures (Ministry of Education), Fudan University, Shanghai 200433, People's Republic of China

E-mail: chunzhen@zzu.edu.cn

Received 25 January 2011, in final form 5 July 2011
Published 27 July 2011
Online at stacks.iop.org/JPhysD/44/325003

Abstract

We theoretically investigate the properties of optical propagation in one-dimensional soft photonic crystals based on ferrofluids using the transfer matrix method. The proposed structure is composed of an alternating ferrofluid layer and a dielectric layer. Ferrofluids are composed of suspended ferromagnetic nanoparticles coated with silver, which has a frequency-dependent dielectric function. Core–shell nanocomposites incorporating an optical signature with magnetic response are particularly useful. The calculated results of dispersion relation show that tunable band gaps can be realized by varying the local magnetic field factor α, the shell thickness parameter t, or the filling fraction ν of the ferrofluid layer. An additional band gap appears in the lower frequency region due to the absorption. These band gaps blue shift when the external magnetic field is enhanced, and red shift when either t or ν is increased. We also extend our analysis to the variation of band width. To meet the requirements of optical devices, such a tunable structure can be used to design optical filters, modulators and waveguides.

(Some figures in this article are in colour only in the electronic version)

1. Introduction

Photonic crystals (PCs) are periodic arrangements of two alternating dielectric layers [1, 2], which were first described independently by Yablonovitch [3] and John [4] in 1987. The unique characteristic of PCs is the existence of a forbidden band, namely a frequency range within which the electromagnetic wave cannot propagate. Until now one-dimensional (1D), two-dimensional and three-dimensional PCs have been widely studied both theoretically and experimentally [5, 6]. Theoretically, the plane wave expansion [7], the transfer matrix [8] and the finite difference time methods [9] have been well developed. Experimentally, the lithography, the self-assembly and the colloidal crystal template methods were developed for fabrication of PCs with well-controlled structures [10]. Generally, the tunable band gaps in PCs can be achieved by the variation of refractive index or the symmetry of materials. Nowadays, using composite microstructures [11] photonic band gaps can be tuned by different external factors such as an electric [12] or magnetic field [13], temperature [14] or mechanical force [15]. Furthermore, the component of PCs is usually a nonabsorbent material, so the wave vector in the system is frequency independent. However, if a metallic part is inserted into the periodic structure, the pathway of the electromagnetic field will be different [16–18]. Here we propose the one-dimensional structure of soft photonic crystals (SPCs) based on ferrofluids considering the absorption effect.

Ferrofluids are a type of colloidal suspension, in which single domain magnetic particles (about 10 nm in diameter) are dispersed in a polar or a nonpolar liquid [19]. They were first manufactured in 1965 by S S Papel. Ferrofluids consist of ferromagnetic suspended particles (such as Co, Fe_3O_4) or ferrimagnetic suspended nanoparticles (such as $CoFe_2O_4$) [20]. Usually, the nanoparticles are coated with a surfactant to prevent their aggregation due to the van der Waals

[3] Author to whom any correspondence should be addressed.

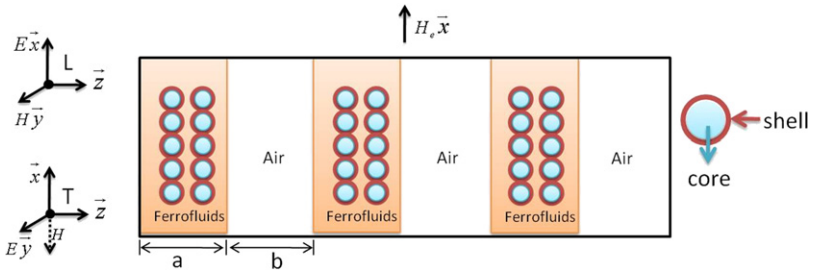

Figure 1. Schematic view of 1D SPCs, composed of an alternating ferrofluid layer and an air layer. For the ferrofluids, the ferromagnetic nanoparticles are suspended in the host liquid. Here we take it as the cobalt nanoparticles (core) coated by silver (shell). When an external magnetic field H_e is applied, the core–shell nanoparticles will align along the magnetic field direction and form chains. An electromagnetic wave is incident on the 1D SPCs along the z-axis, whose electric-field E and magnetic-field H components are directed along the x- and y-axes for the longitudinal (L) field cases, and along the y- and $-x$-direction for the transverse (T) field cases. The thickness of the ferrofluids layer is a. The thickness of the air layer is b. Hence, the lattice constant is $d = a + b$.

and magnetic forces [20, 22–24]. For ionic ferrofluids, the control of pH, ionic strength and counterion nature provide the necessary conditions of stability [20]. Thus, stable ferrofluid suspensions can be affected by the applied magnetic fields, reducing temperature or increasing ionic strength. Using cryogenic TEM, the presence of dipolar chains in ferrofluids without magnetic field was first discovered by Butter *et al* [21]. However, this pre-aggregated unstable state would be disturbed with the appearance of the applied magnetic field. As a result, these nanoparticles will redistribute in the suspension. Finally, they form linear chains. Due to the unique properties of ferrofluids, their wide applications include magneto-optical devices [22, 23, 25], biomedical treatment [26], cancer diagnosis [27] and hypothermal treatment [28].

In this paper, we focus on the complex wave vector in 1D SPCs composed of ferrofluid and dielectric layers. In the studied ferrofluids, the ferromagnetic nanoparticles were taken as Co coated by silver in the host fluid water considering the structure anisotropy induced by the external magnetic field. This SPC structure considering the absorption of the magnetic–plasmonic core–shell nanocomposites is an important extension of our previous work [13]. Through suitable selection of the local magnetic factor α, the shell thickness parameter t and the filling factor ν of the ferrofluid layer, we investigate the tunability of band gaps in the studied 1D SPCs. Also the band width variations are discussed.

2. Formulism

To consider the optical properties of 1D PCs, we mainly focus on the dispersion relation. First, let us take a look at the dispersion relation for the 1D PCs without the metallic layer, namely the wave vector in the PCs is real and frequency independent. In this case, the dispersion relation for electromagnetic waves normally incident on the PCs has the form [8]

$$\cos(k_0 d) = \cos(k_1 a)\cos(k_2 b) - \frac{1}{2}\left(\frac{k_1}{k_2} + \frac{k_2}{k_1}\right)\sin(k_1 a)\sin(k_2 b), \quad (1)$$

where k_0 represents the wave vector in the PCs, $k_1 = \omega n_1/c$ denotes the local wave vector of layer 1 and $k_2 = \omega n_2/c$ is the local wave vector of layer 2; ω is the frequency of light or electromagnetic waves, and c is the speed of light in vacuum; $a(b)$ is the thickness of two alternating layers; $d = a + b$ is the lattice constant. The schematic structure of 1D SPCs is shown in figure 1. It is composed of a ferrofluid layer and an air layer. a is the thickness of the ferrofluid layer, and b is the thickness of air. The filling factor representing the ratio of the ferrofluids in the lattice is defined as $\nu = a/d$. Tunable band gap can be realized in PCs by increasing the refractive index contrast in the constituent materials. For the air layer, the refractive index is 1. To get the largest index contrast we just need to vary the refractive index of the ferrofluids by tuning the magnitude of the applied magnetic field.

In our model system, ferromagnetic linear nanoparticles of linear dielectric constant coated with a nonmagnetic metallic nonlinear shell are investigated in ferrofluids. New nanoparticles (magnetic–metallic composite) combining an optical signature with magnetic response are particularly useful. For the magnetic–nonmetallic shell, they are coated by stabilizing surfactant layers to prevent the aggregation of the nanosized magnetic particles under van der Waals forces. However, the nonmetallic layer potentially reduces the magnetic properties of the magnetic nanoparticles. To investigate the EM wave propagation in this magnetic field induced anisotropic structure, we choose the magnetic–metallic core–shell structure. Metallic coating layer on magnetic nanoparticles is a burgeoning research area because of a simple synthetic procedure and its chemical functionality [26, 29, 30]. Synthesis of metallic (Au, Ag) coated cobalt nanoparticles can be realized by the partial replacement reaction [29]. Through this homogeneous nonaqueous approach, magnetic core–metallic shell composite forms stable ferrofluids.

Now let us introduce the complex wave vector in the 1D SPCs considering the absorption effect. According to the transfer matrix method [31], the dispersion relation now can be expressed as

$$\cos(Kd) = f_1(\omega) + \mathrm{i} f_2(\omega), \quad (2)$$

where K represents the complex wave vector, d is the lattice constant, $f_1(\omega)$ and $f_2(\omega)$ denote the real and imaginary part,

respectively. To get the expression of $f_1(\omega)$ and $f_2(\omega)$, we transform equation (1) as follows:

$$\cos(Kd) = \cos\left(n_1\frac{\omega a}{c}\right)\cos\left(n_2\frac{\omega b}{c}\right) - \frac{1}{2}\left(\frac{n_1}{n_2}+\frac{n_2}{n_1}\right)\sin\left(n_1\frac{\omega a}{c}\right)\sin\left(n_2\frac{\omega b}{c}\right). \quad (3)$$

For the sake of simplicity, we take the dielectric layer 2 as air in our calculation; actually we can also take it as SiO_2, ZnSe, GaAs and so on. Substitute $n_1 = n_r + in_i$, $n_2 = 1$, $\xi_r = \mathrm{Re}(n_1 + \frac{1}{n_1})$ and $\xi_i = \mathrm{Im}(n_1 + \frac{1}{n_1})$ into equation (3). It becomes

$$\cos(Kd) = \cos\left((n_r+in_i)\frac{\omega a}{c}\right)\cos\left(\frac{\omega b}{c}\right) - \frac{1}{2}(\xi_r+i\xi_i)\sin\left((n_r+in_i)\frac{\omega a}{c}\right)\sin\left(\frac{\omega b}{c}\right). \quad (4)$$

Simplifying equation (4), we finally get

$$\cos(Kd) = \left[\cos\left(n_r\frac{\omega a}{c}\right)\cosh\left(n_i\frac{\omega a}{c}\right) - i\sin\left(n_r\frac{\omega a}{c}\right)\sinh\left(n_i\frac{\omega a}{c}\right)\right]\cos\left(\frac{\omega b}{c}\right) - \frac{1}{2}(\xi_r+i\xi_i)\times\sin\left(\frac{\omega b}{c}\right)\left[\sin\left(n_r\frac{\omega a}{c}\right)\cosh\left(n_i\frac{\omega a}{c}\right) + i\cos\left(n_r\frac{\omega a}{c}\right)\sinh\left(n_i\frac{\omega a}{c}\right)\right]. \quad (5)$$

Thus,

$$f_1(\omega) = \cos\left(n_r\frac{\omega a}{c}\right)\cosh\left(n_i\frac{\omega a}{c}\right)\cos\left(\frac{\omega b}{c}\right) - \frac{1}{2}\xi_r\sin\left(\frac{\omega b}{c}\right)\sin\left(n_r\frac{\omega a}{c}\right)\cosh\left(n_i\frac{\omega a}{c}\right) + \frac{1}{2}\xi_i\sin\left(\frac{\omega b}{c}\right)\cos\left(n_r\frac{\omega a}{c}\right)\sinh\left(n_i\frac{\omega a}{c}\right), \quad (6)$$

$$f_2(\omega) = -\sin\left(n_r\frac{\omega a}{c}\right)\sinh\left(n_i\frac{\omega a}{c}\right)\cos\left(\frac{\omega b}{c}\right) - \frac{1}{2}\xi_r\sin\left(\frac{\omega b}{c}\right)\cos\left(n_r\frac{\omega a}{c}\right)\sinh\left(n_i\frac{\omega a}{c}\right) - \frac{1}{2}\xi_i\sin\left(\frac{\omega b}{c}\right)\sin\left(n_r\frac{\omega a}{c}\right)\cosh\left(n_i\frac{\omega a}{c}\right). \quad (7)$$

As we know, the real part of the complex wave vector K, namely k_r, corresponds to the wave number in the 1D SPCs, while the imaginary part k_i determines the absorption coefficient β. It can be expressed as

$$\beta = 2k_i. \quad (8)$$

Simplifying $\cos K$ using $K = k_r + ik_i$ we obtain

$$\cos K = \cos(k_r + ik_i) = \cos k_r\cosh k_i - i\sin k_r\sinh k_i. \quad (9)$$

The real part of the photonic band structure for a given wave number k_r can be found based on equations (2) and (9) by seeking the frequencies which follow the equation

$$\cos(k_r d) = f_1(\omega)\left[\frac{f_2^2(\omega)}{\sin^2(k_r d)}+1\right]^{-1/2}. \quad (10)$$

In our numerical calculations, we take the dielectric constant of silver $\epsilon_1'(\omega)$ as a function of ω. It follows a Drude dielectric function, which is valid for noble metals within the frequency range of interest. $\epsilon_1'(\omega)$ can be expressed as [32]

$$\epsilon_1'(\omega) = \epsilon(\infty) - (\epsilon(0)-\epsilon(\infty))\frac{\omega_p^2}{\omega(\omega+i\gamma)}, \quad (11)$$

where ω_p is the bulk plasmon frequency, $\epsilon(\infty)$ is the high-frequency limit dielectric constant, $\epsilon(0)$ is the static dielectric constant and γ is the collision frequency. Specifically for silver, $\epsilon(\infty) = 5.45$, $\epsilon(0) = 6.18$, and $\omega_p = 1.72\times10^{16}\,\mathrm{rad\,s^{-1}}$ [33]. In addition, we take $\gamma = 0.01\omega_p$ (a typical value for metals). For the cobalt nanoparticle, we take $\epsilon_1'' = -25 + 4i$. It should be reasonable to see that ϵ_1'' is frequency independent, since it only varies very slightly with the frequency of external fields.

Thus, the equivalent linear dielectric constant $\epsilon_1(\omega)$ for the core–shell composite nanoparticle can be obtained through the Maxwell–Garnett formula [34, 35], which describes a two-component composite where many particles of dielectric constant ϵ_p and volume fraction v_p are randomly embedded in a host medium. Thus,

$$\frac{\epsilon_1(\omega)-\epsilon_1'(\omega)}{\epsilon_1(\omega)+2\epsilon_1'(\omega)} = (1-f)\frac{\epsilon_1''-\epsilon_1'(\omega)}{\epsilon_1''+2\epsilon_1'(\omega)}, \quad (12)$$

where f is the volume ratio of the nanoshell to the whole coated nanoparticle. It equals to $f = 1 - r^3/R^3 = 1 - t^3$. The shell thickness parameter $t = r/R$, where r relates to the radius of the magnetic core. R is the radius of the core–shell composites. The thinner the shell layer, the larger the t is. The Maxwell–Garnett formula follows from a well-known asymmetrical effective medium theory, and may thus be valid for a low concentration of nanoparticles in the composites [36].

The effective linear dielectric constant of the whole suspension under present consideration $\epsilon_e(\omega)$ can be given by the developed Maxwell–Garnett approximation which works for suspensions with field-induced anisotropic structures [34]:

$$\frac{\epsilon_e(\omega)-\epsilon_2}{\alpha\epsilon_e(\omega)+(3-\alpha)\epsilon_2} = p\frac{\epsilon_1(\omega)-\epsilon_2}{\epsilon_1(\omega)+2\epsilon_2}, \quad (13)$$

where ϵ_2 is the frequency-independent dielectric constant of the host liquid, and $\epsilon_2 = 1.77$ for water. The volume fraction of the nanoparticles in the suspension is p, and here we take $p = 0.18$. The parameter α measures the degree of structural anisotropy due to the formation of nanoparticle chains, which are induced by the external magnetic field H_e.

The aim of the intended introduction of α into equation (13) is to include the field-induced anisotropy in the system, at least qualitatively. In detail, α denotes the local field factors, $\alpha_\parallel$ and $\alpha_\perp$ for longitudinal and transverse field cases, respectively. Schematic structure of the local magnetic field anisotropy factor $\alpha_\parallel$ and $\alpha_\perp$ is shown in figure 2. Here the longitudinal (or transverse) field case corresponds to the fact that the E-field of the light is parallel (or perpendicular) to the particle chain. There is a sum rule for $\alpha_\parallel$ and $\alpha_\perp$, $\alpha_\parallel + 2\alpha_\perp = 3$. The parameter α measures the degree of anisotropy induced by the applied magnetic field H_e. More precisely, the degree

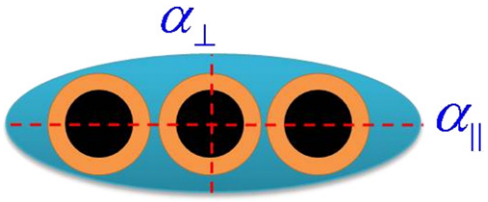

Figure 2. Schematic graph showing the local magnetic factor along the major ($\alpha_\parallel$) or minor axis ($\alpha_\perp$), respectively. The whole nanoparticles chain can be treated as an equivalent spheroid.

of the field-induced anisotropy is measured by how much α deviates from unity, $0 < \alpha_\parallel < 1$ for longitudinal field cases and $1 < \alpha_\perp < 1.5$ for transverse field cases. As H_e increases $\alpha_\parallel$ and $\alpha_\perp$ should tend to 0 and 1.5, respectively, which is indicative of the formation of more and more particle chains as evident in experiments. So a crude estimate of α can be obtained from the contribution of chains, namely $\alpha = \frac{1}{\phi}\sum_{k=1}^{n} kV_0V_k(H_e)N_k$, where ϕ denotes the volume fraction of the structured particles in the suspension, N_k the depolarization factor for a chain with k structured particles, V_0 the volume of one particle in suspension (considered to be spherical and all identical), and $V_k(H_e)$ the density of the chain which is a function of H_e [37, 38]. It is noteworthy that for a given p, $V_k(H_e)$ also depends on the dipolar coupling constant which relates the dipole-dipole interaction energy of two contacting particles to the thermal energy. Specifically, if there is no external magnetic field, $H_e = 0$, the magnetic moments within the ferrofluid particles are randomly distributed, which means no net measurable magnetization can be obtained. It leads to $\alpha_\parallel = \alpha_\perp = 1$. But when an external magnetic field is applied, the magnetic moments of the particles orient along the field direction of the externally applied field. It means the alignment of magnetic moments is very sensitive to the external magnetic field. Therefore, α should be a function of external magnetic fields H_e. As for the refractive index n_1 of the ferrofluid layer, it can be easily obtained from the expression $n_1 = \sqrt{\epsilon_e}$, where ϵ_e is the effective dielectric constant of the ferrofluid layer. Thus, $n_r = \mathrm{Re}(\sqrt{\epsilon_e})$ and $n_i = \mathrm{Im}(\sqrt{\epsilon_e})$.

3. Results and discussions

In our numerical calculations (figures 3–6), the 1D SPCs is composed of alternating ferrofluid and air layers. Specifically, we study cobalt nanoparticles coated by silver. For optical properties in this 1D SPCs, the absorption coefficient β, the dispersion relation $k_r d/\pi$ and the real part $f_1(\omega)$ are considered as a function of frequency $\omega d/2\pi c$ by tuning the local magnetic factor α, the thickness parameter t and the filling factor ν of the ferrofluid layer.

Figure 3 shows the absorption coefficient $\mathrm{Log}_{10}[10^6 \times \beta]$ of 1D SPCs as a function of the frequency $\omega d/2\pi c$. When the external magnetic field H_e is applied, the coated nanoparticles will form chains along the magnetic field direction changing the microstructure of the system accordingly. For the sake of numerical calculations, we take $t = 0.5$ and $\nu = 0.5$. First, we consider the longitudinal (L) field cases as shown in figure 1. When the local magnetic factor $\alpha_\parallel$ gradually

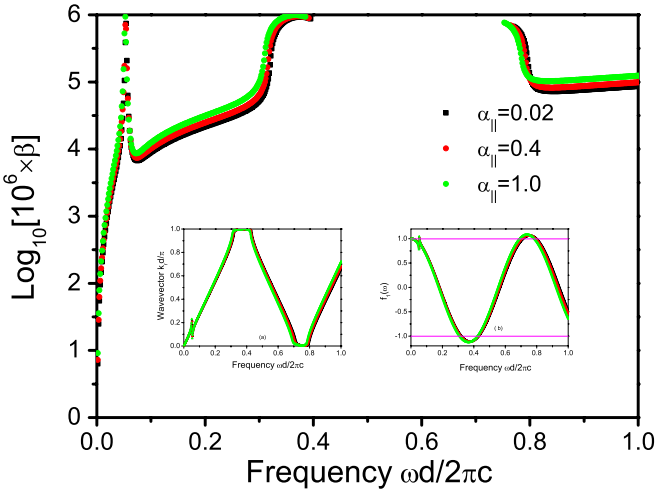

Figure 3. For the L field cases, the absorption coefficient $\mathrm{Log}_{10}[10^6 \times \beta]$ as a function of the frequency $\omega d/2\pi c$ for various $\alpha_\parallel$. Inset (a): dispersion relation of the wave vector $k_r d/\pi$; inset (b): real part of $\cos(Kd)$, namely $f_1(\omega)$. The square, circle and triangular dots correspond to $\alpha_\parallel = 0.02$, 0.4 and 1.0, respectively. Parameters: $t = 0.5$ and $\nu = 0.5$.

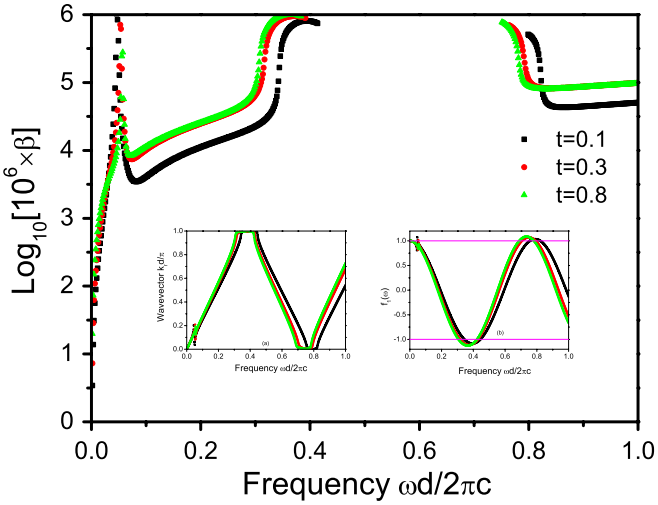

Figure 4. For the L field cases, the absorption coefficient $\mathrm{Log}_{10}[10^6 \times \beta]$ as a function of the frequency $\omega d/2\pi c$ for various t. Inset (a): dispersion relation of the wave vector $k_r d/\pi$; inset (b): real part of $\cos(Kd)$, namely $f_1(\omega)$. The square, circle and triangular dots correspond to $t = 0.1$, 0.3 and 0.8, respectively. Parameters: $\alpha_\parallel = 0.4$ and $\nu = 0.5$.

decreases from 1.0 to 0.02, the structure anisotropy induced by the external magnetic field makes the dispersion curve blue shift (moving to the high-frequency region). Meanwhile the absorption coefficient decreases and the absorption curves are not continuous. To fully understand the origin of such phenomena we can take a look at the insets (a) and (b). Inset (a) shows the real part of the complex wavevector $k_r d/\pi$ as a function of the frequency. An additional band gap appears due to the dissipation coefficient γ in equation (11) in the low-frequency region. Now let us take a look at the distribution of $f_1(\omega)$ as a function of frequency, which is shown as inset (b). It represents the real part of the complex wave vector $\cos(Kd)$, and its oscillation defines the frequency regions in

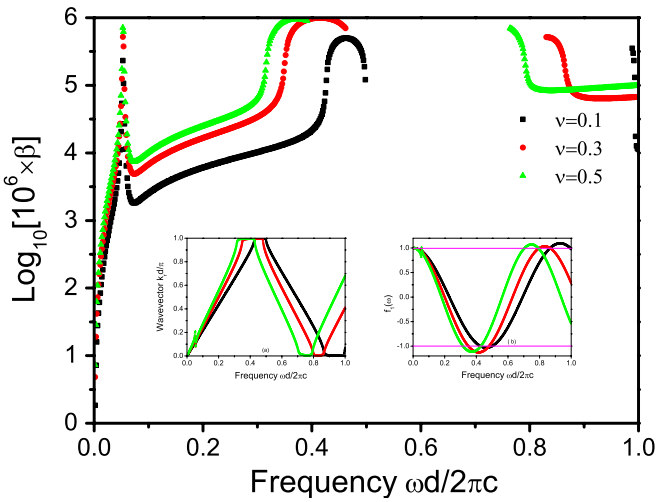

Figure 5. For the L field cases, the absorption coefficient $\mathrm{Log}_{10}[10^6 \times \beta]$ as a function of the frequency $\omega d/2\pi c$ for various ν. Inset (a): dispersion relation of the wave vector $k_r d/\pi$; inset (b): real part of $\cos(Kd)$, namely $f_1(\omega)$. The square, circle and triangular dots correspond to $\nu = 0.1$, 0.3 and 0.5, respectively. Parameters: $\alpha_\parallel = 0.4$ and $t = 0.5$.

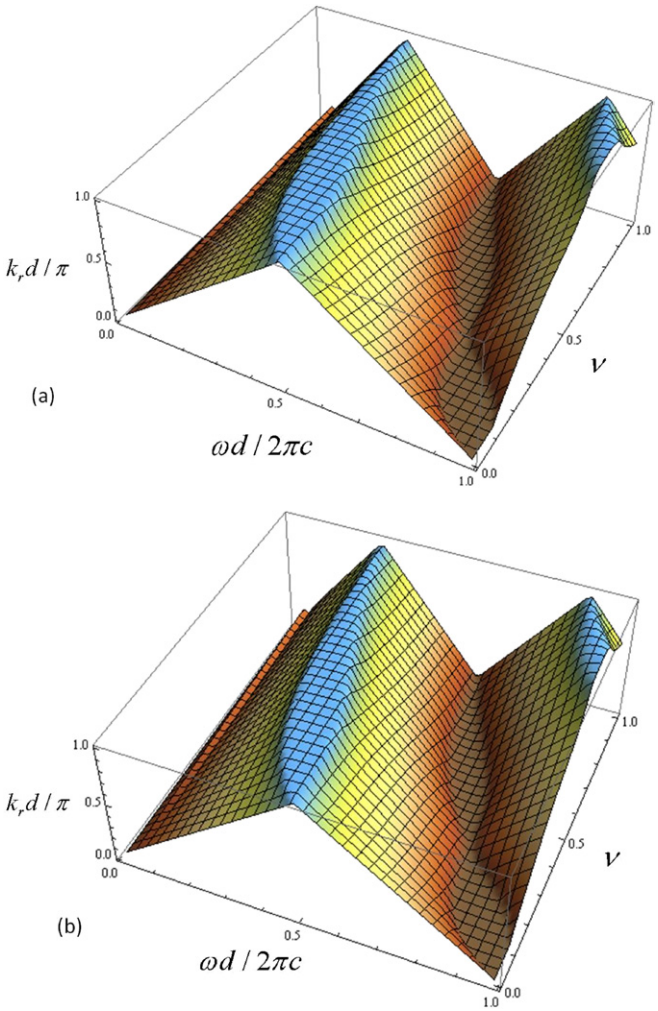

Figure 6. 3D illustration of the dispersion relation $k_r d/\pi$ as a function of the ferrofluid filling fraction ν and frequency $\omega d/2\pi c$. For the filling factor, ν is taken from 0.01 to 1.0. (a) for the L field cases, $\alpha_\parallel = 0.4$; (b) for the T field cases, $\alpha_\perp = 1.2$. Parameter: $t = 0.5$.

which the argument Kd takes real values (the regions where $|f_1(\omega)| \leqslant 1$). In other words, the band gaps happen in the frequency region where $|f_1(\omega)| > 1$. When $\alpha_\parallel$ gradually decreases, the distribution of $f_1(\omega)$ blue shifts (moving to the higher frequency region). For the transverse (T) field cases the behaviours of the dispersion curve are similar to the L field cases (not shown here). Thus, the enhanced magnitude of the external magnetic filed ($\alpha_\parallel$ decreases or $\alpha_\perp$ increases) causes the band gaps of 1D SPCs to blue shift.

Figure 4 demonstrates the absorption coefficient $\mathrm{Log}_{10}[10^6 \times \beta]$ of 1D SPCs as a function of the frequency $\omega d/2\pi c$ depending on the thickness parameter t. For the L field cases, $\alpha_\parallel = 0.4$ and $\nu = 0.5$. When the thickness of the shell increases, t will decrease. From figure 4, one can clearly see that band gaps shift to the low-frequency region when t increases from 0.1 and 0.3 to 0.8. That means, the thinner shell layer of silver gives rise to the redshift of band gaps. Also the larger t leads to higher absorption coefficient $\mathrm{Log}_{10}[10^6 \times \beta]$. Inset (a) illustrates the distribution of $k_r d/\pi$ as a function of frequency. These band gaps in figure 4 are caused by the frequency range where $|f_1(\omega)| > 1$ as shown inset (b).

The influence of filling factor ν on the dispersion curve is illustrated in figure 5. Here we keep the parameters $\alpha_\parallel = 0.4$ and $t = 0.5$. By tuning the filling factor ν from 0.1 and 0.3 to 0.5, we can find a redshift (moving to the low-frequency region) of the band gap of the 1D SPCs as shown in figure 5. It is evident that the absorption coefficient becomes larger when ν increases (figure 5). The distribution of $k_r d/\pi$ and $f_1(\omega)$ are shown as insets (a) and (b), respectively.

We also determined the variation of the band gap width as a function of the local magnetic factor α, the thickness ratio t and the filling factor ν of the ferrofluid layer. The band gap width tends to increase when the magnitude of the local magnetic factor $\alpha_\parallel$ decreases or t increases (not shown here). Specifically, the band gap width variation as a function of filling factor ν is shown in figure 6(a) for the L field case $\alpha_\parallel = 0.4$, $t = 0.5$. ν is taken from 0.0 to 1.0. As we can see, the variation of the second band gap width is closely related to ν. It is gradually getting wider when ν is smaller than 0.35, but when ν is larger than 0.35 the width is reduced. The situation is the same for the T field case as shown in figure 6(b).

Now we give a discussion on the work. As mentioned in [23], aggregation of small nanoparticles occurs spontaneously within ferrofluids to form a linear chain, which happens prior to the formation of linear chains induced by the external magnetic field. And such aggregations are first experimentally observed [21]. Because these magnetic nanoparticles will redistribute in the suspension under the influence of the applied magnetic field, we mainly focus on the stable state of linear chains with applied magnetic field in our model system. Moreover, we take the nanocomposite in a polar liquid (water), but if we change the liquid as a nonpolar liquid (kerosene), the qualitative results in our model system still hold. The only difference in our numerical calculation is to change the value of the dielectric constant of ϵ_2. Meanwhile we assume the

surfactant layer of the nanoparticles has the same dielectric constant as water in our calculation and the interface effect is not considered. For such a core–shell nanocomposite, the presence of the metallic shell on the magnetic core not only provides the unique optical properties on the nanoscale but also makes it possible to functionalize the nanoparticles with other molecules for biomedical research.

4. Conclusions

In summary, based on the transfer matrix method, we theoretically studied the complex wave vector in 1D SPCs, which are composed of periodic ferrofluid layer and air layer. The behaviour in the 1D SPCs is quite different from the real wave vector in the PCs. Numerical results show that structure anisotropy induced by the external magnetic field causes the dispersion curve to blue shift when $\alpha_{\parallel}$ approaches 0.0, or $\alpha_{\perp}$ is close to 1.5. Also by increasing the thickness parameter t and the filling factor ν the band gaps will red shift. These band gaps in this proposed 1D SPCs structure are caused by the oscillating $f_1(\omega)$ within the frequency region where $|f_1(\omega)| > 1$. An additional band gap occurs in the low-frequency region due to the dissipation factor γ in the dielectric function of silver, equation (11). Also the band width variations are calculated. The results presented in this work provide us with a guideline for designing potential photonic devices based on ferrofluids and are helpful in improving their quality.

Acknowledgments

This work is supported by the National Natural Science Foundation of China (No 10974183). JPH acknowledges the financial support by the National Natural Science Foundation of China under Grant Nos 10874025 and 11075035, and by the Chinese National Key Basic Research Special Fund under Grant No 2011CB922004.

References

[1] Joannopoulos J D, Johnson S G, Winn J N and Meade R D 2008 *Photonic Crystals: Molding the Flow of Light* 2nd edn (Princeton, NJ: Princeton University Press)
[2] Joannopoulos J D, Villeneuve P R and Fan S 1997 *Nature* **386** 143
[3] Yablonovitch E 1987 *Phys. Rev. Lett.* **58** 2059
[4] John S 1987 *Phys. Rev. Lett.* **58** 2486
[5] Vlasov Y A, Bo X Z, Sturm J C and Norris D J 2001 *Nature* **414** 289
[6] Fu M, Zhou J and Yu J H 2010 *J. Phys. Chem.* C **114** 9216
[7] Johnson S G and Joannopoulos J D 2001 *Opt. Express* **8** 173
[8] Yeh P 1988 *Optical Waves in Layered Media* (New York: Wiley)
[9] Lonca M, Nedeljkovie D, Doll T, Vuckovic J, Schere A and Pearsall T P 2000 *Appl. Phys. Lett.* **77** 1937
[10] Miyake M, Chen Y C, Braun P V and Wiltzius P 2009 *Adv. Mater.* **21** 3012
[11] Wang S W, Lu W, Chen X S, Li Z F, Shen X C and Wen W J 2003 *J. Appl. Phys.* **93** 9401
[12] Wang G, Huang J P and Yu K W 2008 *Opt. Lett.* **33** 2200
[13] Fan C Z, Wang G and Huang J P 2008 *J. Appl. Phys.* **103** 094107
[14] Debord J D and Lyon L A 2000 *J. Phys. Chem.* B **104** 6327
[15] Park W and Lee J B 2004 *Appl. Phys. Lett.* **85** 4845
[16] Xu X C, Xi Y G, Han D Z, Liu X H, Zi J and Zhu Z Q 2005 *Appl. Phys. Lett.* **86** 091112
[17] Soto-Puebla D, Xiao M and Ramos-Mendieta F 2004 *Phys. Lett.* A **326** 273
[18] Bergmair M and Hingerl K 2007 *J. Opt. A Pure Appl. Opt.* **9** S339
[19] Rosensweig R E 1985 *Ferrohydrodynamics* (New York: Cambridge University Press)
[20] Morais P C, Garg V K, Oliveira A C, Silva L P, Azevedo R B, Silva A M L and Lima E C D 2001 *J. Magn. Magn. Mater.* **225** 37
[21] Butter K, Bomans P H H, Frederik P M, Vroege G J and Philipse A P 2003 *Nature Mater.* **2** 88
[22] Bakuzis A F, Skeff Neto K, Gravina P P, Figueiredo L C, Morais P C, Silva L P, Azevedo R B and Silva O 2004 *Appl. Phys. Lett.* **84** 2355
[23] Eloi M T A, Santos J L Jr, Morais P C and Bakuzis A F 2010 *Phys. Rev.* E **82** 21407
[24] Scherer C and Figueiredo Neto A M 2005 *Braz. J. Phys.* **35** 718
[25] Gao Y, Huang J P, Liu Y M, Gao L, Yu K W and Zhang X 2010 *Phys. Rev. Lett.* **104** 034501
[26] Robinson I, Tung L D, Maenosono S, Wältid C and Thanh N T K 2010 *Nanoscale* **2** 2624
[27] Rahn H, Gomez-Morilla I, Jurgons R, Alexiou C and Odenbach S 2008 *J. Phys.: Condens. Matter* **20** 204152
[28] Gomes J de A, Sousa M H, Tourinho F A, Aquino R, Silva G J da, Depeyrot J, Dubois E and Perzynski R 2008 *J. Phys. Chem.* C **112** 6220
[29] Ban Z and O'Connor C 2004 *Mat. Res. Soc. Symp. Proc.* **818** M5.18
[30] Yu H, Chen M, Rice P M, Wang S X, White R L and Sun S 2005 *Nano Lett.* **5** 379
[31] Kuzmiak V and Maradudin A A 1997 *Phys. Rev.* B **55** 7427
[32] Fan C Z and Huang J P 2006 *Appl. Phys. Lett.* **89** 141906
[33] Kik P G, Maier S A and Atwater H A 2004 *Phys. Rev.* B **69** 045418
[34] Boyd R W 1992 *Nonlinear Optics* (New York: Academic)
[35] Huang J P and Yu K W 2006 *Phys. Rep.* **431** 87
[36] Bergman D J and Stroud D 1992 *Solid State Phys.* **46** 147
[37] Cotae C, Baltag O, Olaru R, Calarasu D and Costandache D 1999 *J. Magn. Magn. Mater.* **201** 394
[38] Pang C P, Hsieh C T and Lue J T 2003 *J. Phys. D: Appl. Phys.* **36** 1764